Hindawi
Journal of Zoological Systematics and Evolutionary Research
Volume 2024, Article ID 8299436, 18 pages
https://doi.org/10.1155/2024/8299436

Research Article

Two New Species of Freshwater Planarian (Platyhelminthes, Tricladida, Dugesiidae, *Dugesia*) from Southern China Exhibit Unusual Karyotypes, with a Discussion on Reproduction in Aneuploid Species

Lei Wang,[1] Shi-Qing Zhu,[1] Fu-Hao Ma,[1] Xiang-Jun Li,[1] Yu-Hao Zhao,[1] Xin-Xin Sun,[1] Ning Li,[1] Ronald Sluys,[2] De-Zeng Liu,[1] Zi-Mei Dong ,[1] and Guang-Wen Chen [1]

[1]*College of Life Science, Henan Normal University, Xinxiang 453007, Henan, China*
[2]*Naturalis Biodiversity Center, Leiden, Netherlands*

Correspondence should be addressed to Zi-Mei Dong; dzmhjx@163.com and Guang-Wen Chen; chengw0183@sina.com

Received 15 October 2022; Revised 13 December 2023; Accepted 26 December 2023; Published 22 February 2024

Academic Editor: Miroslawa Dabert

Two new species of the genus *Dugesia* from Southern China are described by applying an integrative approach, including morphological, karyological, histological, and molecular information. In the molecular phylogenetic tree, the two new species, *Dugesia pendula* Chen & Dong, sp. nov. and *Dugesia musculosa* Chen & Dong, sp. nov., fall into an Eastern Palearctic/Oriental clade and an Oriental/Australasian clade, respectively, while sharing only a rather distant relationship. The separate specific status of the two new species is supported also by their genetic distances. *Dugesia pendula* is characterized by the following features: symmetrical openings of the oviducts into the bursal canal, a duct between seminal vesicle and diaphragm, small diaphragm, dorsally located seminal vesicle, a penis papilla suspended from the dorsal wall of the male atrium, and mixoploid karyotype with diploid complements of $2n = 2x = 14 + 0 - 1$ B-chromosome and triploid complements of $2n = 3x = 21 + 0 - 1$ B-chromosome, with all chromosomes being metacentric. *Dugesia musculosa* is characterized by the following features: asymmetrical openings of the oviducts into the bursal canal; a ventrally displaced ejaculatory duct with a terminal opening; two diaphragms; a bursal canal provided with a strong, thick layer of circular muscle, which extends from the copulatory bursa to the common atrium and gonoduct; the left vas deferens opening at the midlateral wall of the seminal vesicle, while the right sperm duct opens at the dorsolateral wall of the seminal vesicle; and karyotype consisting of complicated diploid and aneuploid mosaicism, with diploid complements of $2n = 2x = 16$ and $2n = 2x = 16 - 1^{7th}\text{-}1^{8th}$, with all chromosomes being metacentric. The uncommon karyotypes, combined with the asexual reproduction of aneuploid animals, are evaluated in the context of the relationship between ploidy levels and reproductive modalities in the genus *Dugesia*.

1. Introduction

Although about 110 species of the freshwater planarian genus *Dugesia* Girard, 1850, have been reported from the major portion of the Old World and Australia, it was only recently that taxonomic studies started to unveil its rich biodiversity in China, which forms a potential distribution hotspot for this genus [1]. From southern China, eight new species were described [2–6], while from northern China, thus far one new species was reported [7]. In the present paper, we add two new species of *Dugesia* to the already-known diversity in southern China by applying an integrative approach, including morphological, karyological, histological, and molecular information.

The uncommon karyotypes of the two new species, combined with the asexual reproduction of aneuploid animals, are evaluated in the context of the relationship between ploidy levels and reproductive modalities in the genus *Dugesia*.

2. Materials and Methods

2.1. Specimen Collection and Culturing. Specimens were collected from under stones in a stream with the help of a paintbrush. At collection, only 10 worms of *D. pendula* Chen & Dong, sp. nov. were collected in the field, none of which was sexually mature. With respect to *D. musculosa* Chen & Dong, sp. nov., over 50 asexual worms and seven sexual worms were collected. After collection, the worms were transferred to plastic bottles filled with stream water that during transportation to the laboratory were placed in a cooler filled with an ice bag.

In an automatic incubator, the planarians were cultured in autoclaved tap water at 20°C and fed with fresh beef liver once per week. The worms were starved for at least seven days before being used for karyotype and histological studies and DNA extraction. Images of their external morphology were obtained by using a digital camera attached to a stereo-dissecting microscope.

2.2. Phylogenetic Analysis and Genetic Distances. Procedures for DNA extraction, amplification, and sequencing followed Wang et al. [5, 7]. Fragments of the cytochrome c oxidase subunit I (COI) and internal transcribed spacer-1 (ITS-1) were amplified using the primer pairs COIF and COIR and 9F and ITSR, respectively [5, 7, 8]. For both of the two new species, four specimens were used to extract DNA, from which COI and ITS-1 were amplified.

In total, 83 sequences of 40 *Dugesia* species from major portions of the geographic range of the genus were used to perform phylogenetic analyses and to calculate genetic distances, including the two new species, while *Schmidtea mediterranea* (Benazzi et al., 1975), *S. polychroa* (Schmidt, 1861), and *Recurva postrema* Sluys & Solà, 2013, were chosen as the outgroup taxa (Table 1). The sequences of *Dugesia* were selected for one or more of the following reasons: (1) they were obtained from representative species from the major geographic range of the genus *Dugesia*; (2) they were obtained from species with a well-established taxonomic status; (3) they were either of high quality and/or had a long length. These sequences—indicated by the species names—are represented as terminals in the phylogenetic trees that we generated.

Sequence analyses were done as described previously by Wang et al. [4–6]. In brief, ITS-1 sequences were aligned online with MAFFT (Online Version 7.247, [9]) using the G-INS-i algorithm. Protein-coding sequences were translated into amino acid sequences in order to check for the presence of stop codons (with the help of the ninth NCBI's genetic code - Flatworm Mitochondrial). With respect to COI sequences, Translator X (http://translatorx.co.uk, [10]) was used, followed by MAFFT with FFT-NS-2 method, was checked by BioEdit 7.2.6.1 [11], and, thereafter, back-translated to nucleotide sequences. Since automated removal of gap columns and variable regions has been reported to negatively affect the accuracy of the inferred phylogeny [12, 13], the Gblocks option [14] was disabled.

Bayesian information criterion (BIC) was implemented in PartitionFinder 2 [15, 16] to estimate the best-fit partition

Table 1: GenBank accession numbers of COI and ITS-1 sequences used in molecular analyses.

Species	GenBank	
	COI	ITS-1
D. adunca	OL505739	OL527659
D. aethiopica	KY498845	KY498785
D. afromontana	KY498846	KY498786
D. arabica	OL410620	OK587374
D. arcadia	KC006971	KC007044
D. ariadnae	KC006972	KC007048
D. batuensis	KF907818	KF907815
D. benazzii	FJ646977 + FJ646933	FJ646890
D. bengalensis	—	FJ646897
D. bifida	KY498851	KY498791
D. bijuga	MH119630	—
D. circumcisa	MZ147041	MZ146782
D. cretica	KC006976	KC007050
D. constrictiva	MZ871766	MZ869023
D. deharvengi	KF907820	KF907817
D. elegans	KC006984	KC007063
D. etrusca	FJ646984 + FJ646939	FJ646898
D. gemmulata	OL632201	—
D. gibberosa	KY498857	KY498803
D. gonocephala	FJ646986 + FJ646941	FJ646901
D. granosa	OL410634	KY498795
D. hepta	FJ646988 + FJ646943	FJ646902
D. japonica	FJ646990	FJ646904
D. liguriensis	FJ646992	FJ646907
D. majuscula	MW533425	MW533591
D. musculosa	OR189184	OR205922
D. naiadis	KF308756	OK587343
D. notogaea	FJ646993 + FJ646945	FJ646908
D. pendula	OR195337	OR205921
D. pustulata	MH119631	OK587366
D. ryukyuensis	AF178311	FJ646910
D. sagitta	KC007006	KC007077
D. semiglobosa	MW525210	MW526992
D. sicula	FJ646994 + FJ646947	DSU84356
D. sigmoides	KY498849	KY498789
D. sinensis	KP401592	—
D. subtentaculata	FJ646995 + FJ646949	DSU84369
D. tumida	OL505740	OL527709
D. umbonata	MT176641	MT177211
D. verrucula	MZ147040	MZ146760
R. postrema	KF308763	—
S. polychroa	FJ646975 + FJ647021	—
S. mediterranea	JF837062	AF047854

schemes and models of the concatenated sequences. The best models for each gene and codon position were GTR + G for ITS-1, GTR + I + G for the first and second codon positions of COI, and HKY + I + G for the third codon position of COI. In the phylogenetic analyses, the concatenated dataset consisted of defined gene partitions. Bayesian inference analysis (BI) was run with MrBayes v3.2 [17] using two replicate runs with four chains for 5 million generations, sampling trees every 1000 generations. The convergence of runs was checked by monitoring that the standard deviation of split-frequencies reached a value below 0.01, thus indicating that the runs had reached stationarity. Following completion of each analysis, the first 25% of the generated trees were discarded as "burn-in," while the remaining trees were used to (a) generate a consensus phylogenetic tree, (b) calculate statistics for the taxon bipartitions, (c) determine values for clade support (posterior probability), and (d) calculate branch lengths. Maximum likelihood (ML) analysis with RaxML 8.2.10 [18] was used to perform 5,000 replicates under the GTRGAMMAI model. BI and ML trees were visualized and edited using Figtree v1.4.3.

The genetic distances of COI and ITS-1 were calculated by MEGA 6.06 [19] with the Kimura 2-parameter substitution model [20, 21]. In order to obtain more accurate values for the genetic distances, COI sequences that had less than 600 bp were removed, since the study of Marques et al. [22] indicated that at least 600 bp of COI needs to be used in the determination of interspecific divergences and for species delineation, at least in the land planarian genus *Obama* Carbayo et al., 2013.

2.3. Histology and Karyology. Histological sections were prepared, as described previously by Dong et al. [23]. In brief, worms were fixed in Bouin's fluid for 24 h, and, subsequently, rinsed and stored in 70% ethanol. For the histological study, specimens were dehydrated in an ascending series of ethanol solutions, after which they were cleared in clove oil and embedded in synthetic wax. Serial sections were made at intervals of 6 μm and were stained with hematoxylin-eosin, or in hematoxylin and Cason's Mallory-Heidenhain stain [24]. Histological preparations of specimens have been deposited in the Zoological Museum of the College of Life Science of Henan Normal University, Xinxiang, China (ZMHNU), and Naturalis Biodiversity Center, Leiden, the Netherlands (RMNH).

Air-drying method was used to obtain karyological preparations, according to the protocols described by Dong et al. [23] and Wang et al. [5]. In brief, 5-10 individuals were randomly selected, with each of the worms being treated separately. Regenerating blastemas were obtained by transversely cutting each worm into 3 fragments (head, middle, and tail), which were cultured for 3 days. After 3 days, 4 blastemas (head, prepharyngeal, post-pharyngeal, and tail) were cut off transversely and placed on 4 separate slides and, thereafter, treated with a 0.02% colchicine solution at 4°C for 3 h. Hereafter, the blastemas were placed in 0.1% KCl hypotonic solution for 3 h. Subsequently, the surplus hypotonic solution was removed from the slides, and then fixative fluid I (glacial acetic acid : absolute alcohol : deionized water in the ratios 3 : 3 : 4) was added and was removed after only a few seconds. Fixative fluid I was then added again for about 30 s, after which the blastemas were evenly hammered with an oversized needle in order to create a cell suspension, which spread over the glass slide. Before the slides were completely dry, fixative fluid II (glacial acetic acid : absolute alcohol as in 1 : 1 proportion) was drop-wise added to the preparations. When the slides had dried again, fixative fluid III (glacial acetic acid) was added for only a few seconds, after which it was removed, and the preparations were dried at room temperature. After 24 h, they were stained for 15 min with a 0.5% Giemsa solution, whereafter the slides were washed with deionized water and dried at room temperature. Hereafter, coverslips were attached with DPX mountant (MFD1266, MesGen Biotechnology Co., Ltd., Shanghai, China).

Mitotic metaphase chromosomes were observed and photographed under a compound microscope (ZEISS, Axio Scope A1) equipped with a CoolCube digital camera (MetaSystems, Altlussheim, Germany). Karyograms were prepared using the IKAROS Karyotyping system (MetaSystems, Altlussheim, Germany, https://metasystems-international.com/en/products/ikaros/). Well-spread sets of metaphase plates from randomly selected individuals (13 from the *D. pendula* population and 25 from the *D. musculosa* population) were used to determine the ploidy level, centromeric indices, and relative lengths of the chromosomes. Based on IKAROS artificial intelligence (AI) for karyotyping, the curved or overlapping chromosomes were accurately measured and their centromeric position was calculated. Hereafter, the relative lengths of the chromosomes and centromeric positions were rechecked by manual calibration. In the calculations of the averages, the very few heteromorphic chromosomes and karyotypes were not included, in order to avoid misleading results and incorrect conclusions. Karyotype parameter measurements were executed as published previously by Chen et al. [25]. Chromosomal nomenclature follows Levan et al. [26].

3. Results

3.1. Molecular Phylogeny and Genetic Distances. Phylogenetic trees were constructed using the alignment of 1418 base pairs (bp), including 774 bp for COI and 644 bp for ITS-1. Four specimens were examined for each of the two new species, *Dugesia pendula* and *D. musculosa*, and these showed no variation in either COI or ITS-1 sequences.

The BI and ML analyses generated trees that showed identical topologies, differing only in support values (Figure 1; Supplementary Figure S1). The Chinese species included in our analysis fall into two major groups, viz., an Eastern Palearctic/Oriental group and an Oriental/Australasian group (pp = 0.99, bs = 77). Five Chinese species (*D. pendula*, *D. tumida* Chen & Sluys, 2022, *D. majuscula* Chen & Dong, 2021, *D. constrictiva* Chen & Dong, 2022, and *D. verrucula* Chen & Dong, 2021), together with *D. japonica* Ichikawa & Kawakatsu, 1964 group into an Eastern Palearctic/Oriental clade. The other seven Chinese species belong to the Oriental/Australasian

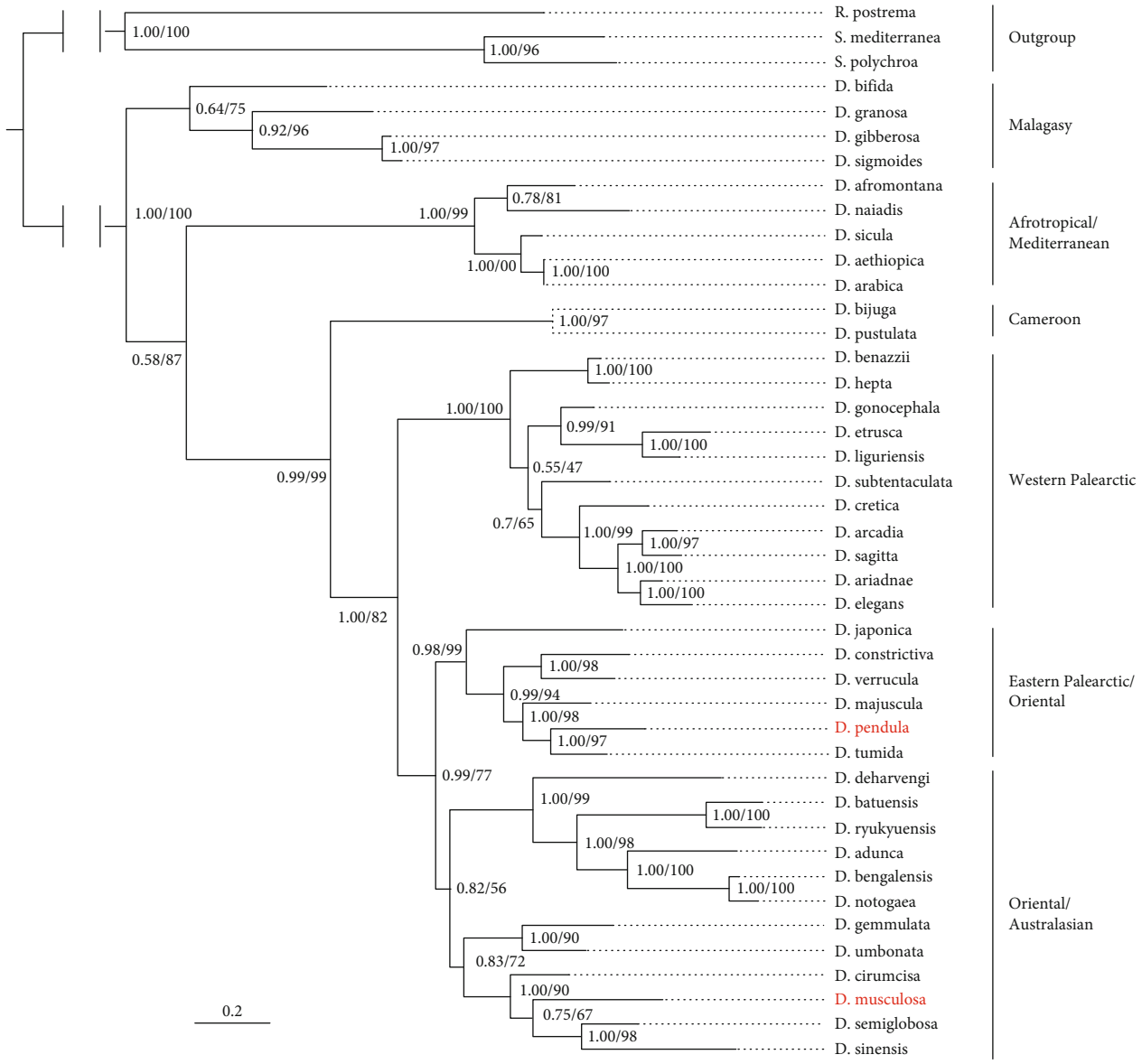

Figure 1: Molecular phylogenetic tree obtained from Bayesian analysis of the ITS-1 and COI concatenated dataset. Numbers at nodes indicate support values (pp/bs). New species indicated in red. Scale bar: substitutions per site.

clade, in which six Chinese species form one subclade (*D. circumcisa* Chen & Dong, 2021, *D. gemmulata* Sun & Wang, 2022, *D. semiglobosa* Chen & Dong, 2021, *D. sinensis* Chen & Wang, 2015, *D. umbonata* Song & Wang, 2020, and *D. musculosa*), while *D. adunca* Chen & Sluys, 2022, belongs to another subclade, albeit with rather low support (pp = 0.82, bs = 56). The two new species described below, *Dugesia pendula* Chen & Dong, sp. nov. and *Dugesia musculosa* Chen & Dong, sp. nov. fall in the Eastern Palearctic/Oriental clade and the Oriental/Australasian clade, respectively, thus sharing only a rather distant relationship. *Dugesia pendula* shares a sister-group relationship with *D. tumida* (pp = 1.00, bs = 97), and together they are sister to *D. majuscula* (pp = 1.00, bs = 98). Together with *D. circumcisa*, *D. gemmulata*, *D. semiglobosa*, *D. sinensis*, and *D. umbonata*, *D. musculosa* forms one of the two major clades within the Oriental/Australasian group. *Dugesia semiglobosa* and *D. sinensis* together are sister to *D. musculosa*, albeit with low support (pp = 0.75, bs = 67). However, the clade of these three species forms the sister taxon of *D. circumcisa* with rather high support (pp = 1.00, bs = 90).

The highest COI distance values between *D. pendula* and *D. musculosa* and their congeners were 22.76% and 23.00% (both with *D. naiadis* Sluys, 2013), respectively, while the lowest COI distance values were 6.07% (*D. pendula* with *D. tumida*) and 12.22% (*D. musculosa* with *D. benazzii* Lepori, 1951), respectively. Furthermore, there is a 16.13% COI difference between the two new species (Supplementary Table S1). With respect to ITS-1, *D. pendula* and *D. musculosa* showed the highest distance values with *D. pustulata* Harrath & Sluys, 2019 and *D. naiadis*, being

17.73% and 19.88%, respectively, and exhibited the lowest distance values with *D. tumida* (1.02%) and *D. circumcisa* (4.83%). For ITS-1, the molecular distance between the two new species was 7.02% (Supplementary Table S2). Thus, the separate species status of *D. pendula* and *D. musculosa* is well-supported by both molecular phylogenetics and genetic distances.

3.2. Systematic Account. Order Tricladida Lang, 1884
Suborder Continenticola Carranza, Littlewood, Clough, Ruiz-Trillo, Baguñà, and Riutort, 1998
Family Dugesiidae Ball, 1974
Genus *Dugesia* Girard, 1850
Dugesia pendula Chen & Dong, sp. nov.
(Figures 2–6)

Zoobank registration: LSID: urn:lsid: https://zoobank.org/NomenclaturalActs/E39C855C-BC90-4F06-846E-BF609CE9E9CE.

Collection site and habitat. On 30th December 2018, the specimens were collected from a stream in the Shiwan Dashan Mountain, close to the China-Vietnam border in Guangxi Zhuang Autonomous Region (Figures 2 and 3(a)), at an altitude of 103 m above sea level (a.s.l.), an air temperature of 14°C, and water temperature of 18.5°C. At collection, none of the worms was sexually mature in the field, yet, in total 13 ex-fissiparous worms sexualized in the laboratory. At this site, only specimens of *D. pendula* appeared to be present, and, thus, no other species was collected at this location. In the population of *D. pendula*, sexual individuals showed no variation in COI and ITS-1, while asexual individuals showed also no variation in COI and ITS-1.

Material examined. Holotype: ZMHNU-LHCA3, Lihuo village (21°37′36″N 107°43′11″E; alt 103 m a.s.l.), Fangcheng County, Guangxi Zhuang Autonomous Region, China, 30 December 2018, coll. G-W. Chen, Z-M. Dong, and L. Wang, sagittal sections on 32 slides.

Paratypes: ZMHNU-LHCA 2, 9, ibid., sagittal sections on 59 and 74 slides, respectively; ZMHNU-LHCA 5 and 6, ibid., horizontal sections on 20 and 14 slides, respectively; ZMHNU-LHCA 7 and 8, ibid., transverse sections on 33 and 49 slides, respectively; RMNH VER. 21023.a, ibid., sagittal sections on 28 slides; RMNH VER. 21023.b, ibid., sagittal sections on 25 slides.

Diagnosis. Dugesia pendula is characterized by the presence of the following features: symmetrical openings of the oviducts into the bursal canal; a long connecting duct between the seminal vesicle and diaphragm; small diaphragm; dorsally located seminal vesicle; penis papilla suspended from the dorsal wall of the male atrium; mixoploid karyotype, with diploid complements of $2n = 2x = 14 + 0 - 1$ B-chromosome and triploid complements of $2n = 3x = 21 + 0 - 1$ B-chromosome, with all chromosomes being metacentric.

Etymology. The specific epithet is derived from the Latin adjective *pendulus*, suspended, pendulous, and alludes to the penis papilla that suspends from the dorsal wall of the male atrium.

Karyology. A total of 140 metaphase plates were examined from six randomly selected specimens, in which 17 had a diploid chromosome portrait of $2n = 2x = 14 + 1$ B-chromosome (Figure 4(a)), 49 showed a triploid complement of $2n = 3x = 21 + 1$ B-chromosome (Figure 4(b)), 8 had a diploid complement of $2n = 2x = 14$ (Figure 4(c)), and 66 exhibited a triploid complement of $2n = 3x = 21$ (Figure 4(d)). In total, 66 metaphase plates exhibited B-chromosomes, while these were absent in 74 complements. Further, there were 25 metaphase plates with diploid complements and 115 triploid complements. Thus, the six specimens examined all exhibited aneuploid plus mixoploid chromosome complements with diploid ($2n = 2x = 14 + 0 - 1$ B-chromosome) and triploid ($2n = 3x = 21 + 0 - 1$ B-chromosome) sets. The haploid sets consisted of seven metacentric chromosomes and no or only one metacentric B-chromosome. A chromosomal plate and idiogram of the karyotype are shown in Figure 4. Karyotype parameters, including relative length, arm ratio, and centromeric index, are given in Table 2.

Description. Sexualized living specimens measured 14-21 mm in length and 1.4-1.6 mm in width. The triangular head is provided with two blunt auricles and two eyes, which are placed in pigment-free spots. Each pigmented eyecup houses numerous photoreceptor cells. The dorsal surface is yellowish-brown, yet the body margin is pale, while accumulations of pigment follow the outline of the pharyngeal pocket (Figure 3(b)); the ventral surface is paler than the dorsal one.

The pharynx is positioned at ca. 4/7 of the body length (as determined from the anterior margin), measuring about 1/6th of the body length (Figure 3(b)); the mouth opening is located at the posterior end of the pharyngeal pocket. Outer pharyngeal musculature is composed of a subepithelial layer of longitudinal muscles, followed by a thin layer of circular muscles; an extra inner layer of longitudinal muscles was not observed. The inner pharyngeal musculature consists of a subepithelial and thick layer of circular muscle, followed by a thin layer of longitudinal muscle.

The hyperplasic, ventrally located ovaries occupy ca. 1/3-1/2 of the dorsoventral space, with several scattered masses situated at a short distance behind the brain. From the ovaries, the infranucleated oviducts run ventrally in a caudal direction to the level of the genital pore, after which they curve dorsomedially to open separately and symmetrically into the ventral portion of the bursal canal (Figure 5). Cyanophil shell glands discharge their secretion into the vaginal region of the bursal canal, at the level of the oviducal openings (Figures 5, 6(a), and 6(b)).

The large, sac-shaped copulatory bursa is situated immediately posterior to the pharynx and occupies ca. 1/2-2/3 of the dorsoventral space (in specimens LHCA 1, 2, 7, and 8), or almost the entire dorsoventral space (in specimens LHCA 3, 4, and 9). The bursa is lined by a stratified, columnar, vacuolated epithelium provided with basal nuclei and is devoid of any surrounding musculature (Figures 5(a) and 6(c)). The bursal canal arises from the posterodorsal wall of the bursa, after which it runs in a caudal direction to the left side of the male copulatory apparatus, whereafter the canal curves ventrad to communicate with the common atrium (Figure 5(a)). The narrow bursal canal is lined with cylindrical, infranucleated, ciliated cells and surrounded by a subepithelial layer

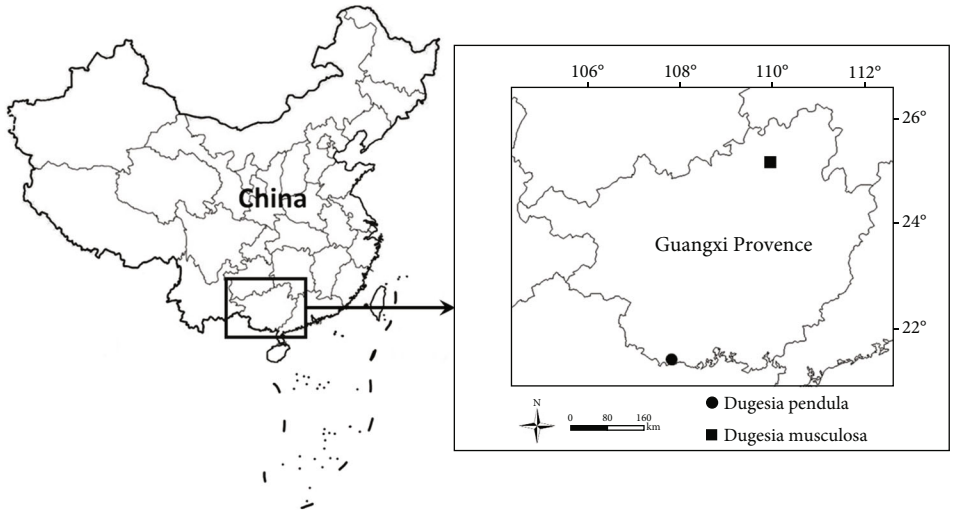

Figure 2: Collection sites of two new species of *Dugesia* in Guangxi Zhuang Autonomous Region, China.

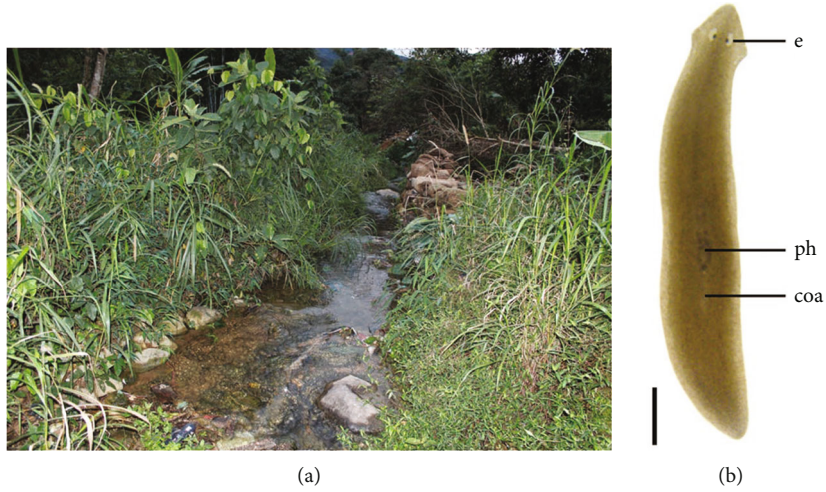

(a) (b)

Figure 3: Habitat and external appearance of *Dugesia pendula*. (a) Sampling site and habitat. (a) Sexually mature, live individual. Scale bar: 2 mm. Abbreviations, coa: copulatory apparatus; e: eye; ph: pharynx.

of longitudinal muscles, followed by a layer of circular muscle. There is an extra outer layer of longitudinal musculature extending from the atrium to halfway along the bursal canal, forming the ectal reinforcement (Figure 5(a)).

The testes are situated dorsally and extend from the level of the hyperplasic ovaries to the posterior end. However, these testicular follicles are poorly developed and contain only small numbers of immature spermatozoa. Therefore, sperm is absent from the vasa deferentia. The sperm ducts are lined with nucleated cells and surrounded by a layer of circular muscles. At the level of the penis bulb, the sperm ducts curve towards the dorsal body surface, then penetrate the ventral wall of the penis bulb to open separately and symmetrically into the midlateral section of the seminal vesicle (Figures 5(b), 6(a), and 6(f)). The penis bulb is located directly anterior to the male atrium and positioned in the dorsal portion of the body; it is rather weakly muscularized. In contrast, the large, sac-shaped seminal vesicle is surrounded by a well-developed layer of intermingled muscle fibres. The seminal vesicle is located in the dorsal body region and is lined by a flat, nucleated epithelium (Figures 5(b) and 6(b)–6(e)).

A well-developed and long duct arises from the posterior wall of the seminal vesicle, after which it runs in a caudal direction, more or less parallel to the body surface. The interconnecting duct is lined with a nucleated epithelium and is surrounded by a thin layer of circular muscles. At the level of the penis papilla this interconnecting duct bends sharply towards the ventral body surface, after which it opens into the ejaculatory duct via a very small diaphragm. The diaphragm and the proximal, dorsal section of the ejaculatory duct receive the abundant secretion of erythrophil penis glands (Figures 5(b) and 6(a)–6(e)). The ejaculatory duct, which is lined with a cuboidal, infranucleated epithelium and is devoid of any discernible musculature, follows a central course through the penis papilla, opening at the

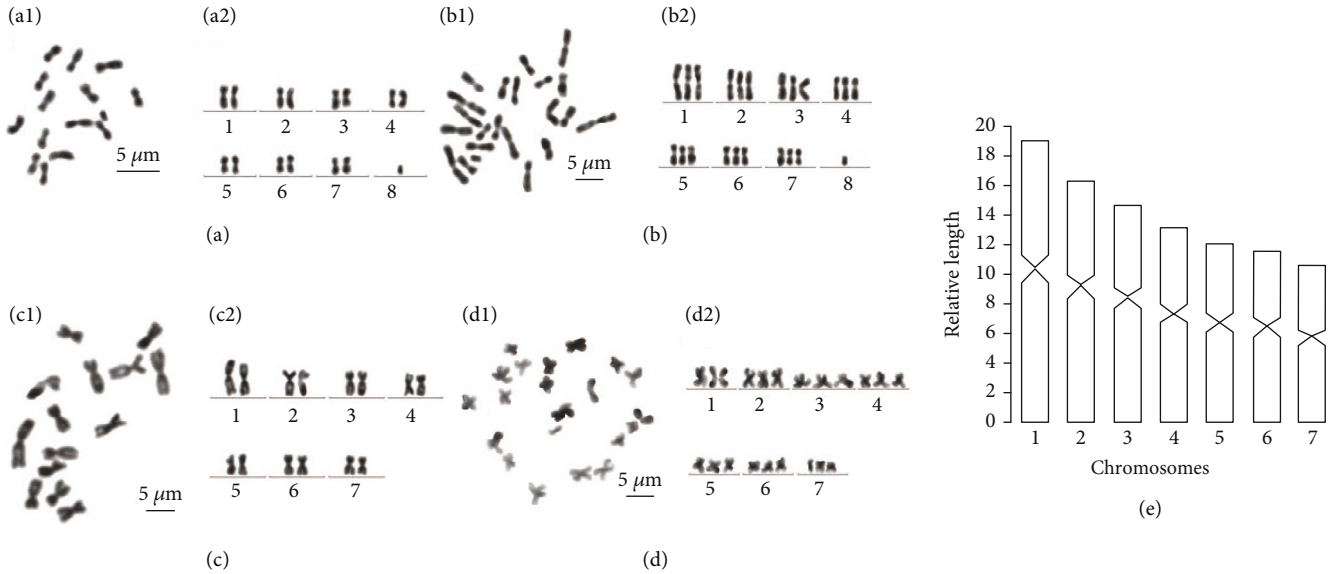

Figure 4: *Dugesia pendula*. (a) (a1, a2) Metaphase plate and karyogram of diploid complement with 1 B-chromosome. (b) (b1, b2) Metaphase plate and karyogram of triploid set with 1 B-chromosome. (c) (c1, c2) Metaphase plate and karyogram of diploid complement. (d) (d1, d2) Metaphase plate and karyogram of triploid set. (e) Idiogram. Scale bar: 5 μm.

tip of the latter (Figures 5(b) and 6). Cyanophil penis glands discharge abundant secretion into the central and distal portion of the ejaculatory duct.

The penis papilla is a cylindrical or barrel-shaped structure that suspends from the dorsal wall of the male atrium and that is covered with an infranucleated epithelium, which is underlain by a subepithelial layer of circular muscle, followed by a layer of longitudinal muscle fibres.

The genital atrium is divided into a common atrium and a male atrium. The common atrium communicates with a gonoduct, which leads to the ventral gonopore; the gonoduct is lined by a tall, columnar epithelium and receives the openings of abundant cement glands (Figures 5, 6(b), 6(c), and 6(e)).

Reproduction. Ten worms were immature at collection, and under laboratory conditions reproduced asexually through the process of fission. But after about 8 months of rearing under laboratory conditions, the immature specimens continuously sexualized. After 12 months of culturing, 13 sexualized worms produced only two cocoons. The spherical cocoons (1.0 mm in diameter) were dark brownish and provided with a stalk, yet no juveniles hatched from these cocoons.

Remarks. Dugesia pendula is unique among its congeners in that it has its penis papilla suspending from the dorsal wall of the male atrium and, thus, the papilla has a fully vertical orientation. This contrasts strongly with the penis papillae in all other species of *Dugesia*, which are generally horizontally or more or less obliquely orientated, pointing in a ventrocaudal direction. A species that somewhat resembles *D. pendula* in the vertical orientation of the penis papilla is *D. krishnaswamyi* Kawakatsu, 1975, from India. However, in *D. krishnaswamyi*, the short penis papilla still has a slightly oblique, ventrocaudal orientation, while the penis bulb is very large and extends onto two large atrial folds [27], which are absent in *D. pendula*. Furthermore, *D. krishnaswamyi* is a blackish-brown species, in contrast to the yellowish-brown *D. pendula*.

In some specimens of *D. nannophallus* Ball, 1970, the penis papilla seemingly exhibits a vertical orientation [28]. However, this is only due to the fact that the penis papilla of this species is highly asymmetrical, with a large dorsal lip and a small ventral lip, which contrasts with the symmetrical papilla of *D. pendula*.

Notably, *D. pendula*, *D. tumida*, and *D. majuscula* belong to a small clade in the phylogenetic tree (Figure 2), although each species occupies its own branch, while they are anatomically very different. In both of the two last-mentioned species, the ejaculatory duct has a subterminal, dorsal opening at the tip of the penis papilla. Furthermore, *D. tumida* possesses a symmetrical penial valve at the base of the penis papilla, while in *D. majuscula*, the posterior section of the bursal canal is expanded. All of these features are absent in *D. pendula*.

Dugesia musculosa Chen & Dong, sp. nov.

(Figures 2 and 7–11)

Zoobank registration: LSID: urn:lsid: https://zoobank.org/NomenclaturalActs/165761d2-71c9-4a4d-8660-55579462825c.

Collection site and habitat. On 7th April 2021, specimens were collected from a stream on the Southern Tianpin Mountain, Guangxi Zhuang Autonomous Region (Figures 2 and 7(a)), at an altitude of 237 m a.s.l.; the air temperature was 18°C and the water temperature was 14°C. At collection, approximately seven worms were sexual, while most of the worms were asexual in the field. Under laboratory conditions, the asexual worms were fissiparous, of which 5 ex-fissiparous specimens sexualized. Two other species were found at the same location from where *D. musculosa* was collected. However, these three species could be distinguished

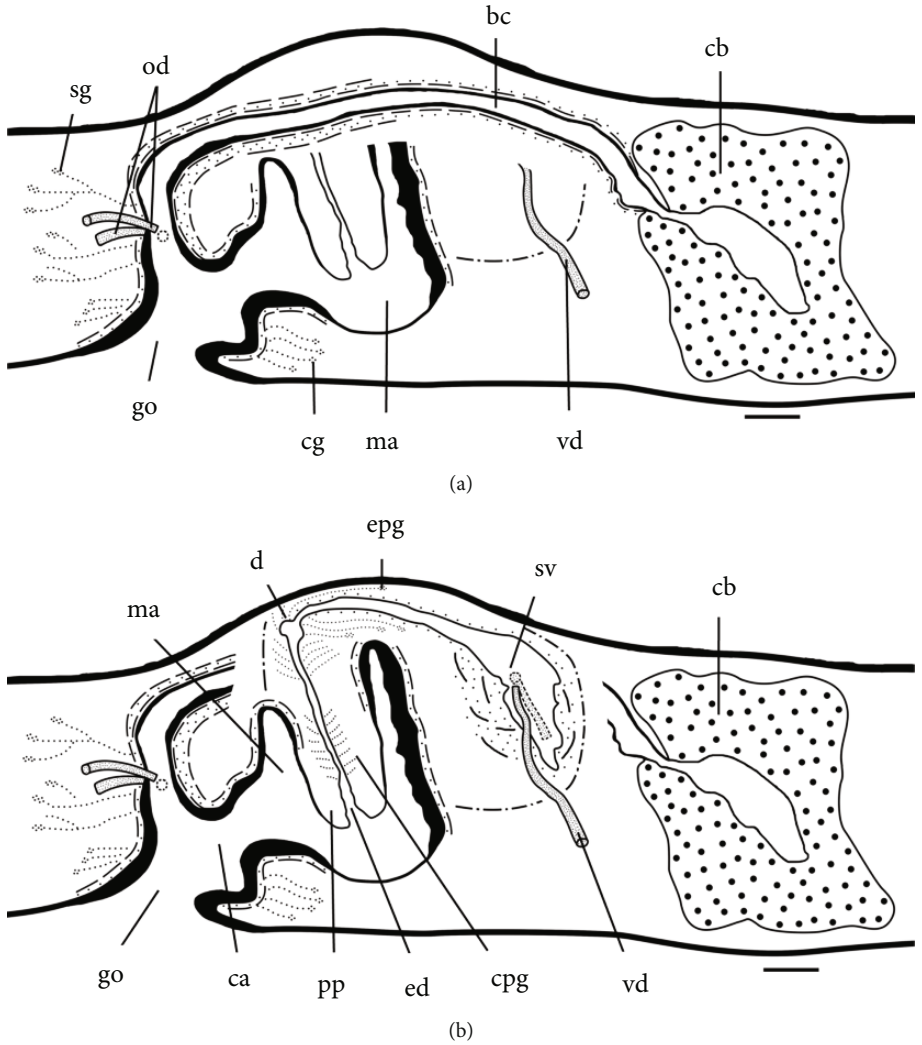

Figure 5: *Dugesia pendula*. Sagittal reconstruction of the copulatory apparatus of holotype LHCA3. (a) Female copulatory apparatus. (b) Male copulatory apparatus. Scale bar: 100 μm. Abbreviations: bc: bursal canal; ca: common atrium; cb: copulatory bursa; cg: cement glands; cpg: cyanophil penis glands; d: diaphragm; ed: ejaculatory duct; epg: erythrophil penis glands; go: gonopore; ma: male atrium; od: oviduct; pp: penis papilla; sg: shell glands; sv: seminal vesicle; vd: vas deferens.

from each other by morphology, histology, and molecular data. Specimens labelled as YFHXA represented *D. musculosa*, while specimens YFXHB concerned an unidentified *Dugesia* species (as the animals are still asexual), and YFHXC involved another new species (approximately November 2022, ex-fissiparous individuals sexualized and laid infertile cocoons). With respect to the population of *D. musculosa*, sexual individuals showed no variation in COI and ITS-1, while asexual individuals showed also no variation in COI and ITS-1.

Material examined. *Holotype*: ZMHNU-YFXHA4, Xihe village (25°5′30″N 109°43′33″E), alt. 237 m a.s.l., Yongfu County, Guangxi Zhuang Autonomous Region, China, 7 April 2021, coll. Z-M. Dong, F. Wu, and Y-X. Wang, sagittal sections on 41 slides.

Paratypes: ZMHNU-YFXHA 1, 2, 5, 9, and 10, ibid., sagittal sections on 38, 26, 24, 33, and 33 slides, respectively; ZMHNU-YFXHA8, ibid., transverse sections on 45 slides; ZMHNU-YFXHA7, ibid., horizontal sections on 20 slides; RMNH VER. 21024.a, ibid., sagittal sections on 35 slides; RMNH VER. 21024.b, ibid., sagittal sections on 35 slides.

Diagnosis. *Dugesia musculosa* is characterized by the presence of the following features: oviducts following highly asymmetrical trajectories before separately opening into the bursal canal; two diaphragms; a bursal canal provided with a highly powerful and thick layer of circular muscles, which extends from the copulatory bursa to its opening into the common atrium but also surrounds the common atrium and the gonoduct; left vas deferens opening into the midlateral section of the seminal vesicle, and the right sperm duct opening into the dorsolateral portion of the vesicle; karyotype exhibiting complicated aneuploid and diploid mosaicism ($2n = 2x = 16$ and $2n = 2x = 16 - 1^{7th}\text{-}1^{8th}$), with the haploid chromosome number being 8, and all chromosomes being metacentric.

Etymology. The specific epithet is derived from the Latin adjective *musculosus*, muscular, and alludes to the highly

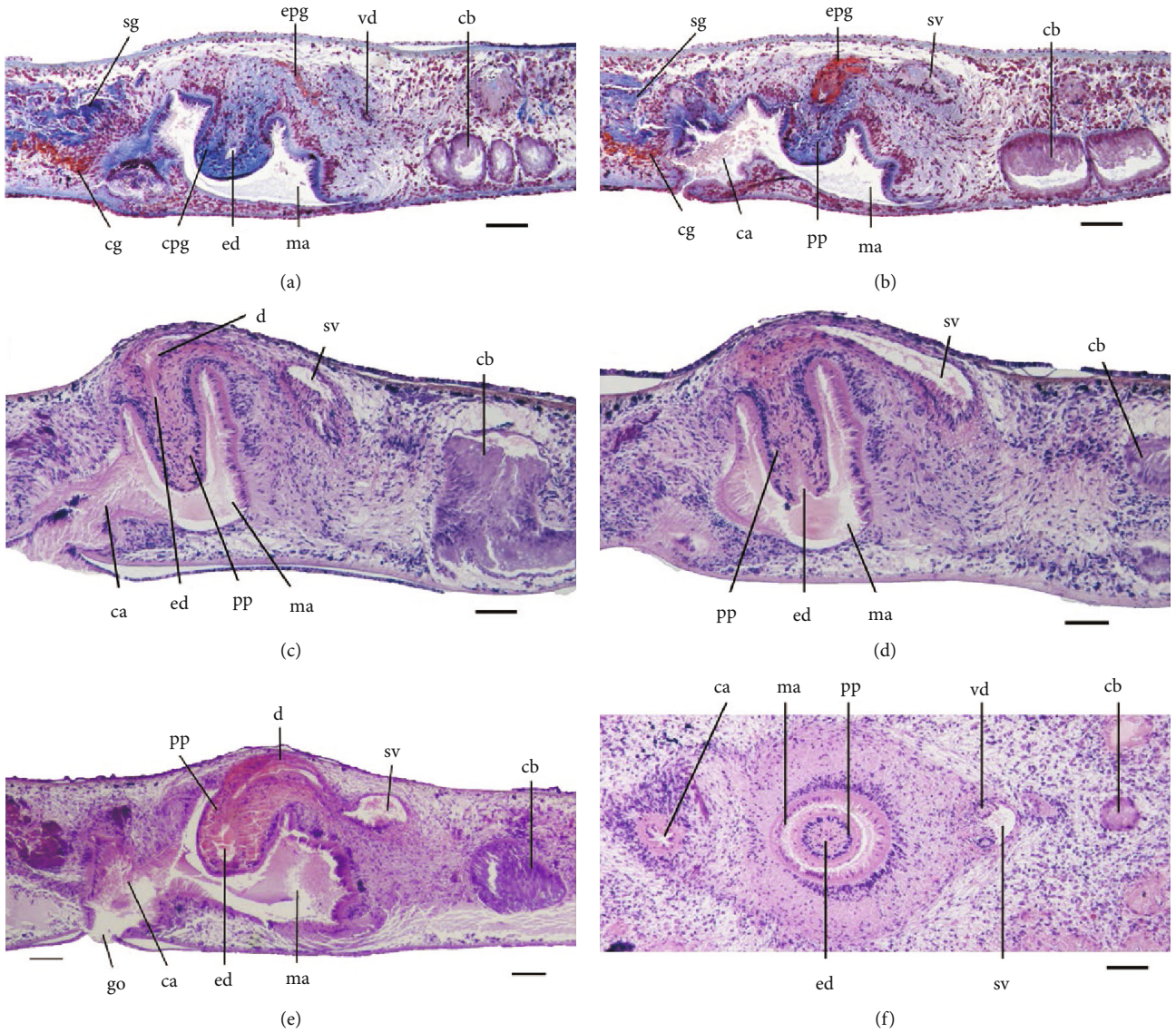

FIGURE 6: *Dugesia pendula*. Photomicrographs of sagittal (a–e) and horizontal (f) sections. (a, b) Paratype ZMHNU-LHCA2, showing suspended penis papilla and seminal vesicle. (c, d) Holotype ZMHNU-LHCA3, showing suspended penis papilla, seminal vesicle, diaphragm, and copulatory bursa. (e) Paratype ZMHNU-LHCA9, showing suspended penis papilla, copulatory bursa, diaphragm, and seminal vesicle. (f) Paratype ZMHNU-LHCA5, showing suspended penis papilla, seminal vesicle, and ejaculatory duct. Scale bars: 100 μm. Abbreviations: see the caption of Figure 5.

powerful and thick layer of circular muscle on bursal canal, common atrium, and gonoduct.

Karyology. From eight randomly selected specimens, a total of 141 metaphase plates were examined, in which 86 metaphase plates showed an aneuploid karyotype with 14 chromosomes (each of the chromosomes pairs 7 and 8 lost one chromosome, Figure 8(a)), and 46 plates had a diploid complement of $2n = 2x = 16$ (Figure 8(b)), while the remaining 5 metaphase plates could not be determined and 4 heteromorphic metaphase plates exhibited irregular aneuploid karyotypes. All eight specimens exhibited complicated karyotypes, with diploid complements of 16 chromosomes and aneuploid complements of 14 chromosomes (7^{th} and 8^{th} chromosomes lost), while all chromosomes were metacentric. Thus, all of the eight specimens examined showed complicated aneuploid and diploid mosaicism, with 8 being the haploid chromosome number. A chromosomal plate and the idiogram of this karyotype are shown in Figure 8. Karyotype parameters, including relative length, arm ratio, and centromeric index, are given in Table 3.

Description. Sexualized living specimens measured 14-18 mm in length and 1.3-1.8 mm in width. The triangular head is provided with two blunt auricles and two eyes, which are placed in pigment-free spots. Each pigmented eyecup houses numerous photoreceptor cells. The dorsal surface is dark-brown, with accumulations of pigment following the outline of the pharyngeal pocket, while the body margin is pale; the ventral surface is paler than the dorsal surface (Figure 7(b)).

The pharynx is positioned approximately at the mid-region of the body, measuring about $1/6^{th}$ of the body length

Table 2: Karyotype parameters (mean values and standard deviations) of *Dugesia pendula*.

Chromosome	Relative length	Arm ratio	Centromeric index	Chromosome type
1	19.09 ± 1.55	1.20 ± 0.10	45.55 ± 1.92	m
2	16.56 ± 1.14	1.27 ± 0.14	44.24 ± 2.46	m
3	14.69 ± 0.74	1.38 ± 0.14	42.30 ± 2.09	m
4	13.24 ± 0.47	1.31 ± 0.17	43.82 ± 2.89	m
5	12.14 ± 0.74	1.29 ± 0.15	43.90 ± 2.98	m
6	11.60 ± 0.97	1.31 ± 0.10	43.38 ± 2.04	m
7	10.69 ± 0.83	1.21 ± 0.05	45.24 ± 1.58	m

m: metacentric.

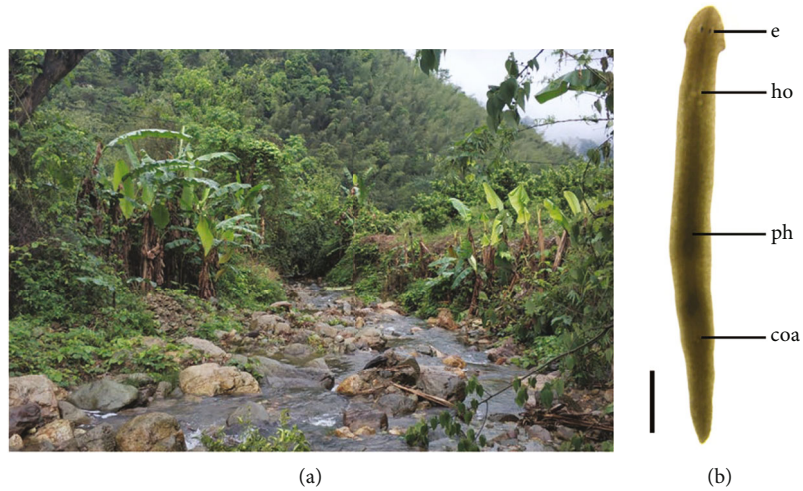

Figure 7: *Dugesia musculosa*. Habitat and external appearance. (a) Sampling site and habitat. (b) Sexually mature, live individual. Scale bar: 2 mm. Abbreviations: ho: hyperplasic ovaries; for other abbreviations, see caption of Figure 3.

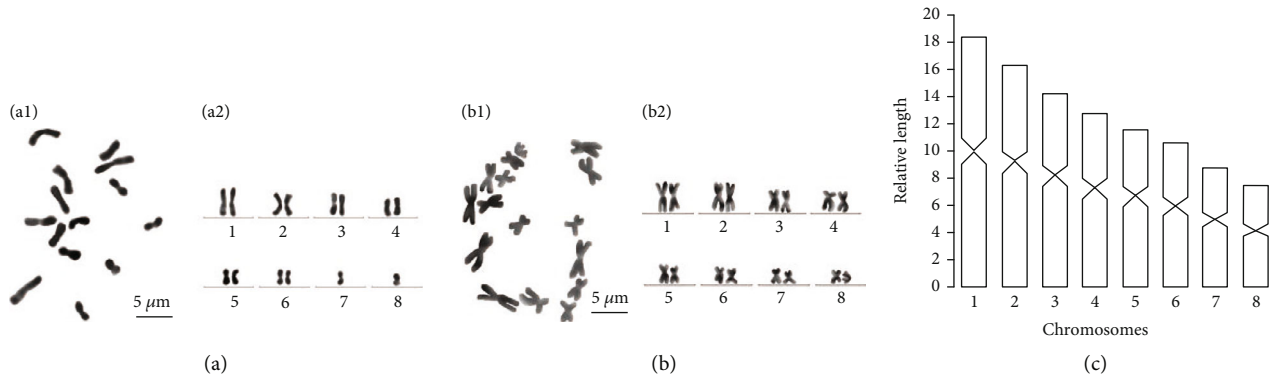

Figure 8: *Dugesia musculosa*. (a) (a1, a2) metaphase plate and karyogram of diploid complement with 14 metacentric chromosomes (missing one 7th and one 8th chromosome). (b) (b1, b2) metaphase plate and karyogram of diploid complement with 16 metacentric chromosomes. (c) Idiogram. Scale bar: 5 μm.

(Figure 7(b)). The mouth opening is located at the posterior end of the pharyngeal pocket. Outer pharyngeal musculature is composed of a subepithelial layer of longitudinal muscles, followed by a thin layer of circular muscles; an extra inner layer of longitudinal muscles was not observed. The inner pharyngeal musculature consists of a subepithelial and thick layer of circular muscle fibres, followed by a thin layer of longitudinal muscle.

The hyperplasic ovaries occupy more than half of the dorsoventral space, with several scattered masses situated at a short distance behind the brain. From the ovaries, the oviducts run ventrally in a caudal direction. From about the level of the gonopore, the two ducts follow rather different trajectories. From thereon, the right oviduct curves medio-dorsally, and upon reaching the dorsal section of the body, it recurves in anterior direction, whereafter it

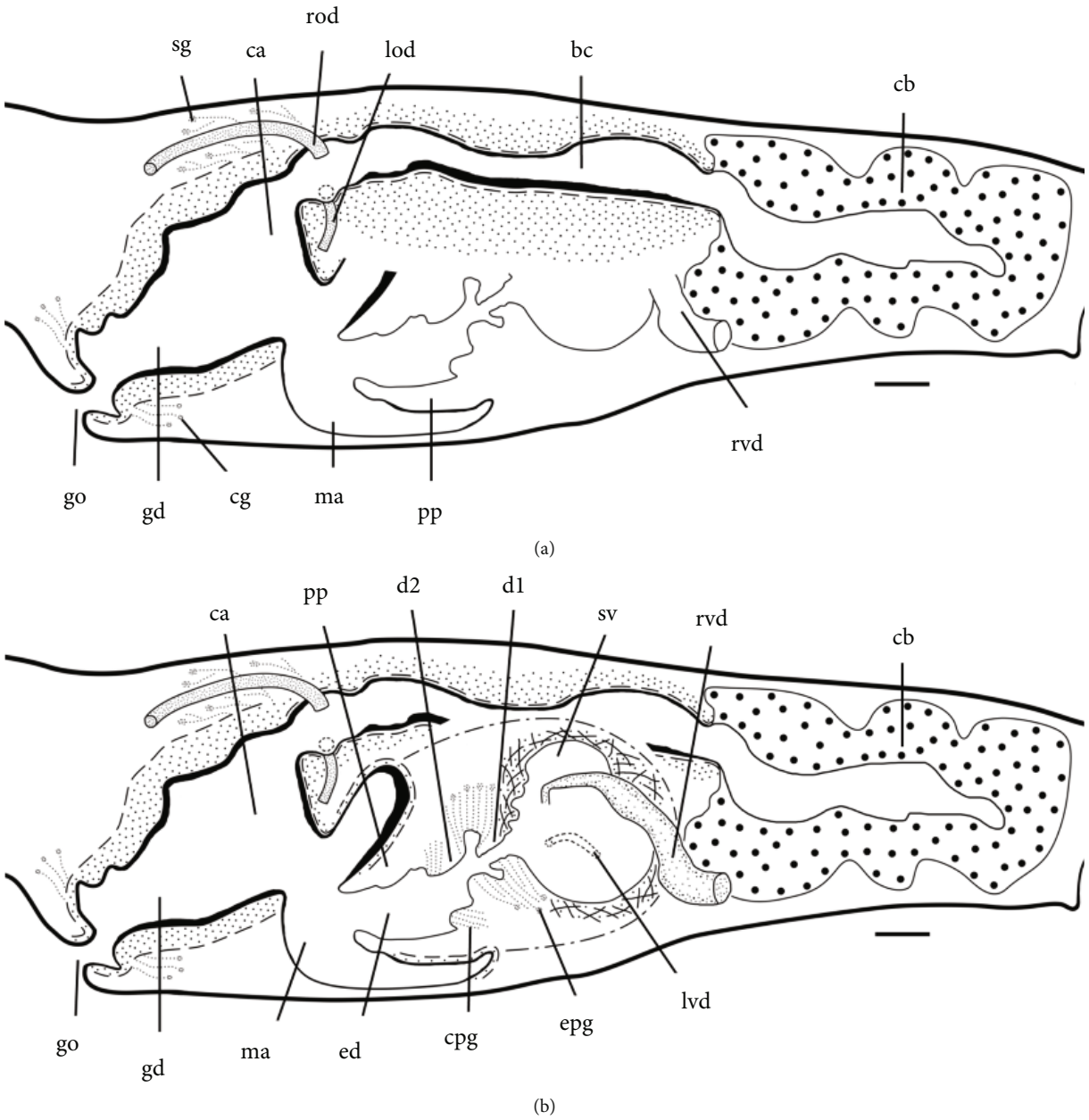

Figure 9: *Dugesia musculosa*. Sagittal reconstruction of the copulatory apparatus of holotype ZMHNU-YFXHA4. (a) Female copulatory apparatus. (b) Male copulatory apparatus. Scale bar: 100 μm. Abbreviations: bc: bursal canal; ca: common atrium; cb: copulatory bursa; cg: cement glands; cpg: cyanophil penis glands; d: diaphragm; ed: ejaculatory duct; epg: erythrophil penis glands; gd: gonoduct; go: gonopore; lod: left oviduct; lvd: left vas deferens; ma: male atrium; pp: penis papilla; rod: right oviduct; rvd: right vas deferens; sg: shell glands; sv: seminal vesicle.

curves downwards to open into the posterior section of the bursal canal, near its point of communication with the common atrium. Thus, the oviduct approaches the bursal canal from a dorsal direction. In contrast, at the level of the gonopore, the left oviduct immediately starts to recurve in an anteromedial direction and approaches the ventral side of the bursal canal, into which it opens at a point that lies even closer to the opening of the bursal canal into the common atrium (Figures 9 and 10(a)). Cyanophil shell glands discharge their secretion into the vaginal region of the bursal canal around the oviducal openings (Figure 9).

A large, sac-shaped copulatory bursa is situated immediately behind the pharynx, extending backwards over a distance of about 600-800 μm, while occupying most of the dorsoventral space (Figures 9 and 10(c)). The bursa is lined by a stratified, columnar, vacuolated epithelium that is provided with basal nuclei and is devoid of any surrounding musculature. The bursal canal arises from the midposterior wall of the bursa, and, thereafter, immediately expands in diameter to become a wide or even very wide duct, which runs in a caudal direction to the left side of the male copulatory apparatus. The posterior section of the bursal canal

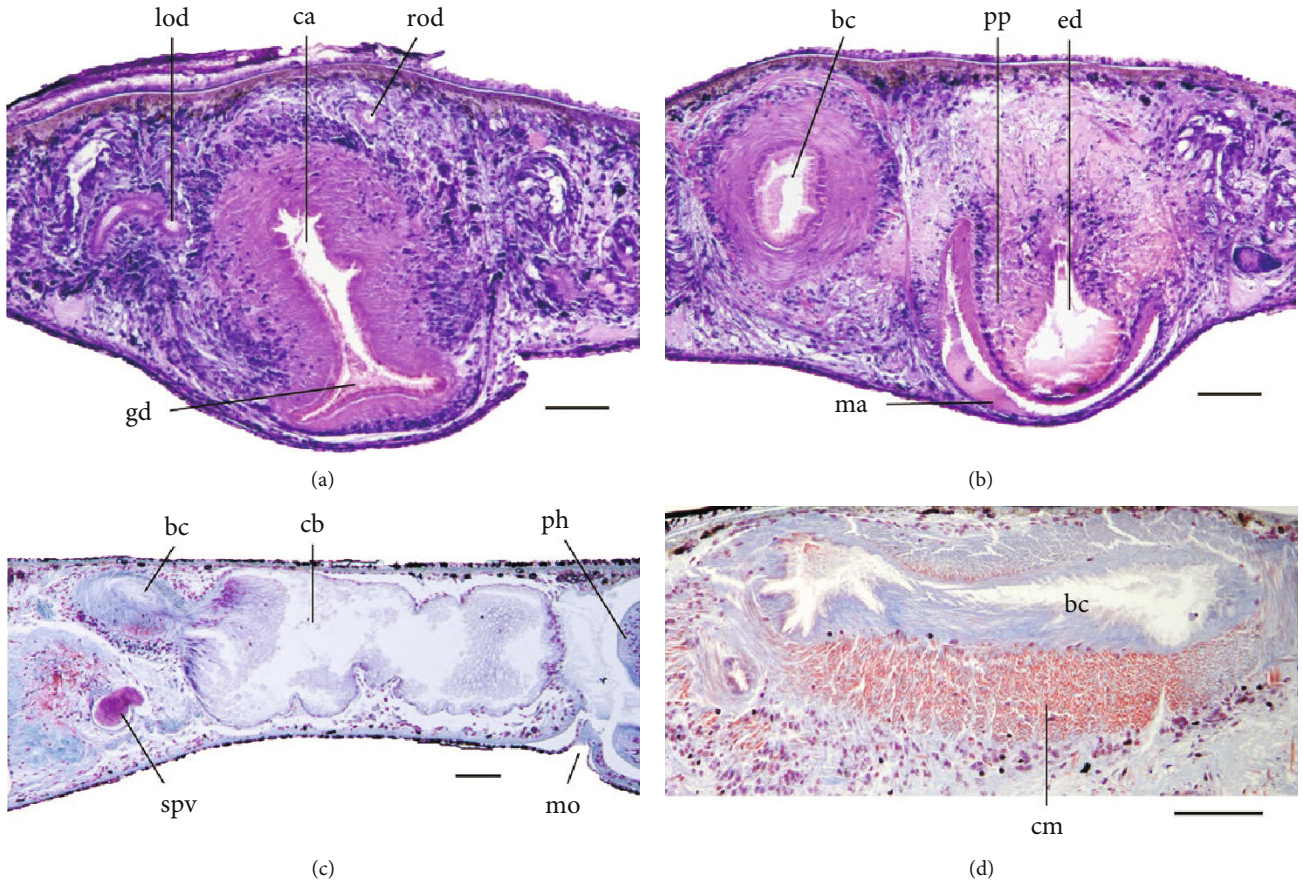

Figure 10: *Dugesia musculosa*. Photomicrographs of transverse (a, b) and sagittal (c, d) sections. (a, b) Paratype ZMHNU-YFXHA8, showing asymmetrical openings of oviducts, well-developed circular muscles around common atrium and gonoduct, penis papilla, and ejaculatory duct. (c) Paratype ZMHNU-YFXHA9, showing large copulatory bursa. (d) Holotype ZMHNU-YFXHA4, showing bursal canal with thick coat of circular muscle. Scale bars: 100 μm. Abbreviations: cm: circular muscles; mo: mouth; spv: spermiducal vesicle; for other abbreviations, see caption of Figure 9.

curves ventrad to open into the broad common atrium (Figure 9). The bursal canal is lined with cylindrical, infranucleated, ciliated cells and surrounded by a subepithelial, thin layer of longitudinal muscles, followed by a very thick layer of circular muscle (Figures 9, 10(b), 11(a), and 11(b)), which measures about 70-100 μm in thickness on the ventral side of the bursal canal, and 45-63 μm on its dorsal side. This highly powerful and thick layer of circular muscle extends along the bursal canal from the copulatory bursa to the common atrium and even encompasses the gonoduct (Figures 9, 10(a), 10(d), 11(c)–11(e)).

The dorsal testes are well-developed and provided with numerous mature spermatozoa and extend from the level of the hyperplasic ovaries to the posterior end of the body. At the level of the copulatory bursa, the vasa deferentia expand to form spermiducal vesicles, which are packed with sperm. At the level of the penis bulb, the sperm ducts curve dorsomedially, penetrate the penis bulb, and open separately into the posterior, distal portion of the seminal vesicle. The left sperm duct penetrates the posterolateral wall of the penis bulb to open into the midlateral portion of the seminal vesicle. The right sperm duct bends towards the dorsal body surface, and after recurving ventrad, it penetrates the anterodorsal wall of the penis bulb to open into the laterodorsal portion of the seminal vesicle (Figures 9(b), 11(a), and 11(b)). Thus, the sperm ducts open somewhat asymmetrically into the seminal vesicle.

The large, sac-shaped seminal vesicle is lined by a flat, nucleated epithelium and is surrounded by a layer of irregularly crosswise arranged muscle fibres, forming a kind of loose net that extends throughout the major portion of the penis bulb, the latter occupying most of the dorsoventral space (Figures 9(b), 11(e), and 11(f)). The seminal vesicle opens into the ejaculatory duct via two diaphragms, the first one being pointed and the second diaphragm being a blunt structure located more distally in the ejaculatory duct. Both diaphragms receive the openings of erythrophil penis glands (Figures 9(b) and 11(f)), while cyanophil glands discharge their secretion into a section of the ejaculatory duct immediately posterior to the second diaphragm. The wide ejaculatory duct opens at the tip of the penis papilla. The broad, conical penis papilla is covered with an infranucleated epithelium, which is underlain by a subepithelial layer of circular muscle, followed by a layer of longitudinal muscle fibres.

The penis papilla lies in a spacious male atrium that via a constriction opens into a large common atrium, the latter

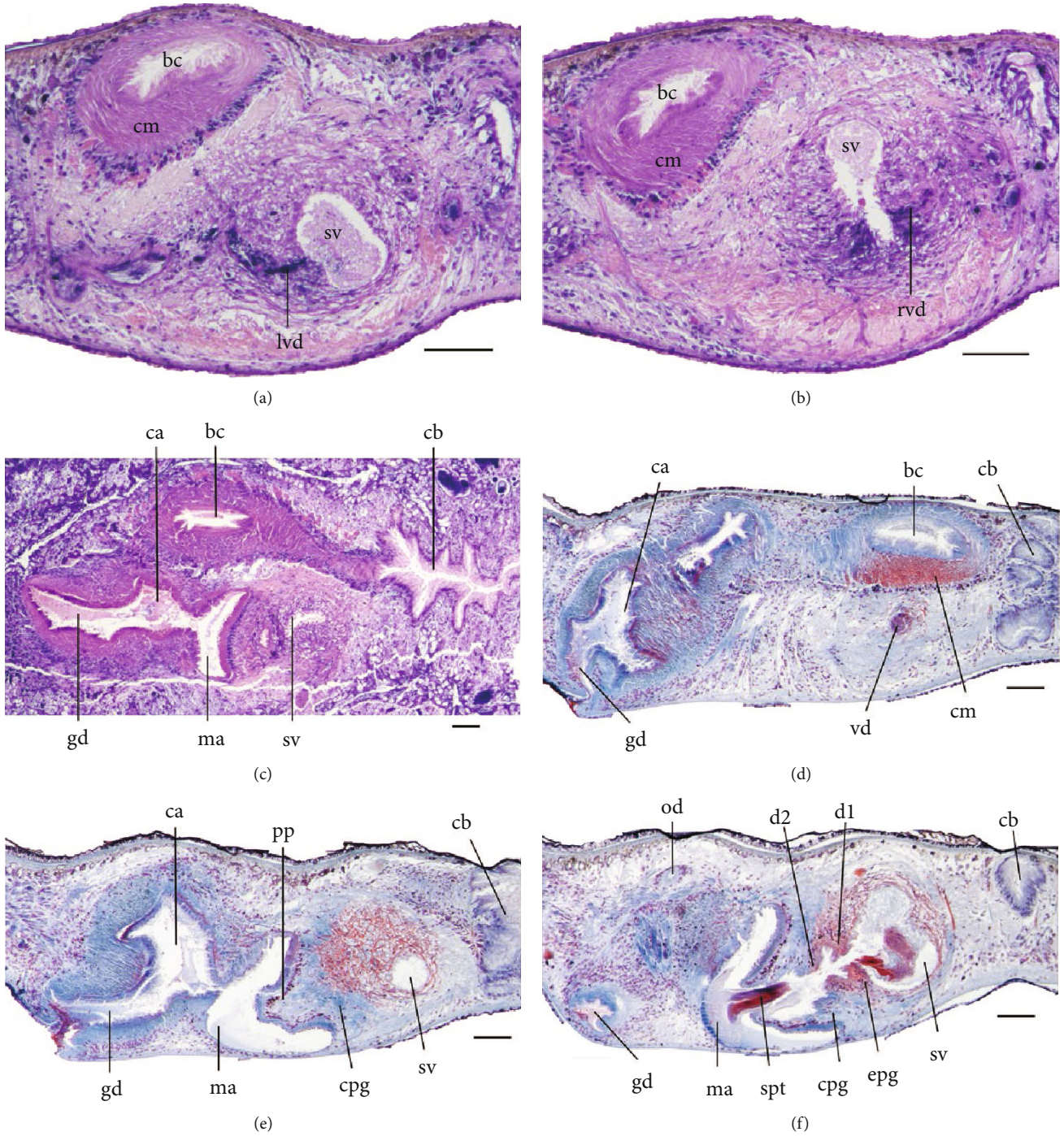

Figure 11: *Dugesia musculosa*. Photomicrographs of transverse (a, b), horizontal (c), and sagittal (d–f) sections. (a, b) Paratype ZMHNU-YFXHA8, showing asymmetrical openings sperm ducts and well-developed circular muscles around bursal canal. (c) Paratype ZMHNU-YFXHA7, showing well-developed circular muscles around bursal canal and gonoduct. (d) Holotype ZMHNU-YFXHA4, showing well-developed circular muscles around bursal canal and gonoduct. (e) Holotype ZMHNU-YFXHA4, showing penis papilla and seminal vesicle. (f) Holotype ZMHNU-YFXHA4, showing penis papilla, wide ejaculatory duct, large seminal vesicle, two diaphragms, and spermatophore. Scale bars: 100 μm. Abbreviations: spt, spermatophore; for other abbreviations, see captions of Figures 9 and 10.

communicating with a pronounced and long gonoduct. Both gonoduct and common atrium are lined with a columnar epithelium, which is underlain by a thick layer of circular muscle (Figures 9, 10(a), and 11(c)–11(f)). The gonoduct leads to the ventral gonopore and receives the openings of erythrophil cement glands.

Reproduction. Numerous asexual worms, seven mature worms, and two cocoons were collected in the field and

Table 3: Karyotype parameters (mean values and standard deviations) of *Dugesia musculosa*.

Chromosome	Relative length	Arm ratio	Centromeric index	Chromosome type
1	18.38 ± 1.26	1.19 ± 0.22	45.93 ± 2.43	m
2	16.28 ± 0.73	1.30 ± 0.19	45.17 ± 2.61	m
3	14.22 ± 0.67	1.36 ± 0.20	42.90 ± 2.38	m
4	12.77 ± 0.85	1.34 ± 0.15	43.63 ± 1.50	m
5	11.56 ± 0.64	1.38 ± 0.14	42.54 ± 1.64	m
6	10.54 ± 0.56	1.31 ± 0.16	43.67 ± 1.92	m
7	8.73 ± 1.66	1.32 ± 0.15	43.70 ± 1.97	m
8	7.52 ± 1.65	1.23 ± 0.15	45.41 ± 1.43	m

m: metacentric.

brought back to the laboratory. After about 1 month of rearing under laboratory conditions, 5 immature specimens sexualized. During the laboratory culture, none of the mature animals (sexual at collection or sexualized during culturing) produced any cocoons.

Remarks. Dugesia musculosa exhibits a combination of a number of features that sets it immediately apart from all of its congeners, in particular, the presence of (a) a bursal canal provided with a highly powerful and thick layer of circular muscles, which extends from the copulatory bursa to its opening into the common atrium but also surrounds the common atrium and the gonoduct, (b) two diaphragms, and (c) oviducts following highly asymmetrical trajectories before separately opening into the bursal canal.

There are several other species of *Dugesia* that exhibit a highly muscularized bursal canal, such as *D. afromontana* Stocchino & Sluys, 2012, *D. batuensis* Ball, 1970, *D. capensis* Sluys, 2007, *D. gibberosa* Stocchino & Sluys, 2017, and *D. granosa* Stocchino & Sluys, 2017. However, in none of these species, the circular muscle layer reaches the thickness of that of *D. musculosa*, while in these species the strong musculature does not extend onto the common atrium and the gonoduct. In some species of *Dugesia*, only a portion of the bursal canal is strongly muscularized. For example, in *D. japonica*, the vaginal region is surrounded by a hump of mesenchymal tissue traversed by several rows of longitudinal and circular muscle fibres [29–31], while in *D. mertoni* (Steinmann, 1914), only the proximal section of bursal canal, near the vaginal region, has a thick coat of circular muscles [32]. In contrast, in *D. musculosa*, the entire bursal canal is enveloped by an extremely thick musculature.

The presence of two diaphragms is a rare condition among species of *Dugesia* and is found in only seven congeners, viz., *D. bijuga* Harrath & Sluys, 2019, *D. circumcisa*, *D. didiaphragma* De Vries, 1988, *D. machadoi* de Beauchamp, 1952, *D. maghrebiana* Stocchino et al., 2009, *D. mirabilis* De Vries, 1988, and *D. semiglobosa* [4, 5, and references therein]. It is interesting to note that two of these species are closely related to *D. musculosa*, viz., *D. circumcisa* and *D. semiglobosa*, as these belong to the same clade in our phylogenetic tree (Figure 1). However, each species occupies its own branch, while they are anatomically very different. For example, *D. circumcisa* shows a nozzle at the tip of the penis papilla, while *D. semiglobosa* exhibits a curious copulatory bursa lined with a complex stratified epithelium, features that are absent in *D. musculosa*.

Dugesia bijuga is only very distantly related to *D. musculosa* (Figure 1) and is also very different from the latter, in that, it possesses a highly glandular, barrel-shaped penis papilla and lacks the highly powerful and thick layer of circular muscles on the bursal canal, common atrium, and gonoduct. Similar to the situation in *D. musculosa*, the seminal vesicle of *D. didiaphragma* is surrounded also by a thick layer of intermingled musculature, but the gross morphology of its copulatory apparatus is rather different. Lastly, *D. maghrebiana* differs from *D. musculosa* in that its penis papilla is asymmetrical and is also provided with a knob-like extension.

In species of *Dugesia*, the left and right sperm ducts usually open symmetrically into the seminal vesicle. An exception is formed by *D. circumcisa*, in which the left sperm duct opens dorsally to the right one, which differs from the situation in *D. musculosa*. It is only in *D. bifida* Stocchino & Sluys, 2014, where the right sperm duct opens into the seminal vesicle dorsally to the left one, similar to the situation in *D. musculosa*. However, *D. bifida* is easily distinguished from *D. musculosa* by the peculiar course of its oviducts, which give rise to a common posterior extension [33].

4. Discussion

Molecular phylogenetic trees of previous studies showed that the Afrotropical/Mediterranean and Malagasy groups generally occupy basal positions in the phylogenetic tree of the genus *Dugesia* and that the Western Palearctic group shares a sister-group relationship with the Eastern Palearctic/Oriental/Australasian group [3–5, 7, 34], which basically agrees with the topology of our present tree (Figure 1). In the analyses of Stocchino et al. [34] and Song et al. [3], the Malagasy species did not form the branch that was sister to all other *Dugesia* included in the study, albeit with low support. In their tree, it was an Afrotropical/Mediterranean group that formed the sister group to all other *Dugesia* species included in the analysis.

Unfortunately, the amount of molecular data available for species of *Dugesia* is rather limited, while the number

of presently known species for China is low. This leads to the situation that many known species of *Dugesia* cannot be represented in molecular phylogenetic trees. In turn, this causes several nodes to have low support values in BI and ML trees (Figure 1; Supplementary Figure S1), resulting in less stable relationships among Malagasy, Afrotropical (including Cameroon), and Mediterranean species. However, in the most recent historical-biogeographic analysis of the genus *Dugesia*, it was shown that the situation is even more complex, in that there are two separate Malagasy clades [1]. In other words, Malagasy lineages do not form a single monophyletic group, with one of these Malagasy clades being sister to all other *Dugesia* species. The other Malagasy clade was sister to an Afrotropical-Eastern Mediterranean clade, which together shared a sister-group relationship with four major clades from the Afrotropics, Asia, Eastern Europe + Middle East, and Western Europe [1]. For Oriental, Australasian, and Eastern Palearctic species of *Dugesia*, our BI and ML analyses generated trees with identical topologies, with only very few nodes being weakly supported. Furthermore, the taxonomic status of the two new species described herein is well-supported by molecular phylogenetics, thus complementing the anatomical evaluation.

The separate specific status of the two new species is supported also by their genetic distances. *Dugesia pendula* showed the lowest COI and ITS-1 distances with *D. tumida*, being 6.07% and 1.02%, respectively. *Dugesia musculosa* showed the lowest COI and ITS-1 distances with *D. benazzii* and *D. circumcisa*, being 12.22% and 4.83%, respectively. The COI and ITS-1 distances between the two new species were 16.13% and 7.02%, respectively. According to previous studies of the genus *Dugesia*, the lowest COI interspecific distance among species is commonly greater than 6%, while the lowest ITS-1 distance is usually more than 1% [6, 7 and references therein]. Thus, based on these markers, the two new species are well-separated not only from their congeners but also from each other.

In *Dugesia* species, the basic chromosome number concerns three types, viz., 7, 8, and 9 [35], with 8 being most frequent and 7 and 9 much rarer. Therefore, *D. pendula* shares its basic number of 7 chromosomes only with *D. hepta* Pala, Casu, & Vacca, 1981, *D. batuensis*, and *D. ryukyuensis* Kawakatsu, 1976 [29, 36–38]. However, in *D. pendula*, all chromosomes are metacentric, whereas *D. batuensis* exhibits 6 metacentric chromosomes and one subtelocentric chromosome, and *D. ryukyuensis* shows 6 metacentric chromosomes and one submetacentric chromosome, which is the case also in *D. hepta* [38–40]. Furthermore, *D. pendula* exhibits an aneuploid plus mixoploid karyotype with diploid ($2n = 2x = 14 + 0 - 1$ B-chromosome) and triploid ($2n = 3x = 21 + 0 - 1$ B-chromosome) sets, thus contrasting with the chromosome complements of the other species. For only many populations of *D. ryukyuensis*, B-chromosomes or mixoploidy have been reported. With respect to *D. musculosa*, its complex aneuploid (missing a 7^{th} and 8^{th} chromosome) plus diploid sets with a basic number of 8 metacentric chromosomes represents a karyotype that thus far has not been reported for any other species of *Dugesia* or even for any member of the Dugesiidae.

In species of *Dugesia*, the presence of B-chromosomes and monosomic chromosomes are generally considered to represent a case of aneuploidy. Apart from the situation in *D. pendula*, the presence of B-chromosomes and, thus, the condition of aneuploidy have been reported also for several other species of *Dugesia*, viz., *D. aethiopica* Stocchino, Manconi, Corso & Pala, 2002, *D. benazzii* Lepori, 1951, *D. etrusca* Benazzi, 1944, and *D. maghrebiana* and many populations of *D. ryukyuensis*, *D.sicula*, *D. arabica* Harrath & Sluys, 2013, and *D. japonica* [35, 41–48].

However, the karyotypes of these species are rather different, so the condition of aneuploidy and the presence of B-chromosomes are actually expressed in greatly different chromosome portraits. For example, in *D. arabica*, *D. sicula*, and *D. ryukyuensis*, B-chromosomes are part of a triploid karyotype, while in *D. maghrebiana*, *D. aethiopica*, and *D. pendula*, they form a component of a mixoploid karyotype. Further, it is noteworthy that the condition of aneuploidy is found in all three of the haploid karyotypes with either a basic chromosome number of 7, 8, or 9.

The karyotype of *D. musculosa* exhibits a complex diploid set ($2n = 2x = 16$ and $16\text{-}7^{th}\text{-}8^{th}$), with a basic chromosome number of 8. We surmise that this represents a case of aneuploidy with a monosomic condition. A similar case of diploid aneuploidy has been reported for one population of *D. ryukyuensis*, in which only one chromosome was absent [43]. Furthermore, monosomy is also found in several populations of *D. japonica* and *D. ryukyuensis*, which exhibit triploid aneuploidy (loss of one or more chromosomes) [43]. Furthermore, B-chromosomes were also observed in *D. japonica* and *D. ryukyuensis* populations [43].

In the genus *Dugesia*, populations of several species show other cases in which chromosomes are absent. For instance, one population belonging to *D. gonocephala* s. str. (Dugès, 1830) exhibited aneuploidy, with the majority of cells possessing 24 chromosomes, but some cells containing 23 or 25 chromosomes [49]. Individual fissiparous specimens of *D. aethiopica* showed two complements, viz., $27 + 1 - 2$ B-chromosome and $18 \pm 1 + 0 - 1$ B-chromosomes [35]. Presently, it is difficult to formulate a good explanation for the abovementioned complex and aneuploid karyotypes (with certain chromosomes being absent), albeit that frequent occurrence of both mixoploidy and aneuploidy in *Dugesia* populations has been postulated to form an adaptive response to environmental pressures [35].

With respect to reproduction, aneuploid populations generally reproduce asexually by means of fission [35 and references therein]. Recent studies of freshwater planarians showed that many individuals of *D. subtentaculata* s. s. (Draparnaud, 1801) present very high genetic levels of mosaicism due to their fissiparous reproduction [50]. High levels of karyotypic mosaicism are present in *D. pendula* and *D. musculosa.* Fissiparous reproduction may allow planarians to endure situations of unbalanced karyotypes, as during periods of fissiparous reproduction individuals do not undergo meiosis and, thus, would not suffer from selection against chromosomal rearrangements [51]. Furthermore, high chromosome number in *D. pendula* (diploidy plus triploidy) is accompanied by a loss of sexual

reproduction, a phenomenon that was reported also for three other species of freshwater planarian, viz., *Phagocata vitta* (Dugès, 1830), *Polycelis felina* (Dalyell, 1814), and *Crenobia alpina* (Dana, 1766) [52]. However, a reduction in chromosome number apparently leads also to loss of sexual reproduction, at least in *D. musculosa.*

When ex-fissiparous animals sexualize, either under laboratory conditions or in the field, they generally exhibit poorly developed testes and hyperplasic ovaries, which is precisely the case in *D. pendula*, with its mixoploid and aneuploid chromosome complement. However, during the sexualization process, mixoploid individuals may be able to reconstitute the original diploid karyotype and, thus, become capable of sexual reproduction, a situation that has been reported for several mixoploid populations of *D. japonica*, one mixoploid population of *D. gonocephala* s. str., and also in *D. adunca* [6, 35, 49]. Such mixoploid, fertile specimens represent examples of gonado-somato-mosaicism, with the gonads having a ploidy level and a chromosomal development enabling successful sexual reproduction [53].

The presence of well-developed testes in sexualized, fertile specimens resembles the situation of normal sexual reproduction in species of *Dugesia*. Although we failed to find cocoons, we did encounter sexual animals in the population of *D. musculosa*. Nevertheless, in the laboratory, we observed in this species only fissiparous reproduction. In both sexual and sexualized ex-fissiparous specimens of *D. musculosa*, well-developed testes were present as well as hyperplasic ovaries. The presence of such hyperplasic ovaries is remarkable because generally, these ovaries coincide with abnormal oocytes, which causes infertility [6, 46, 54]. Such sexualized specimens with well-developed testes and hyperplasic ovaries have been reported for several specimens of *D. semiglobosa* as well as ex-fissiparous specimens of *D. majuscula,* which produce either infertile cocoons or reproduce by fission [5]. Our present results suggest that in *D. musculosa*, the aneuploid chromosome complement (reduction in chromosome number), accompanied by hyperplasic ovaries, interferes with successful sexual reproduction, at least in the laboratory.

Data Availability

Holotypes and paratypes of the two new species were deposited in the Zoological Museum of the College of Life Science of Henan Normal University, Xinxiang, China (ZMHNU), and Naturalis Biodiversity Center, Leiden, the Netherlands (RMNH). Newly generated DNA sequences were deposited in GenBank (Table 1).

Ethical Approval

All handling procedures were strictly compliant with the current Animal Protection Law of China. This study did not involve endangered or protected species. No approvals were required for collections of specimens from the locations in this study. Ethical approvals are not required at Henan Normal University, Xinxiang University, or Naturalis Biodiversity Center for research conducted on invertebrates such as flatworms used in this study.

Conflicts of Interest

The authors declare that they have no conflict of interest.

Authors' Contributions

Guang-Wen Chen and Zi-Mei Dong conceived and designed the study. Guang-Wen Chen, Zi-Mei Dong, and Lei Wang sampled the specimens. Lei Wang and Xiang-Jun Li made the histological sections. Guang-Wen Chen, Zi-Mei Dong, Lei Wang, De-Zeng Liu, and Ronald Sluys analysed the histological sections. Lei Wang prepared the reconstruction drawings. Lei Wang, Shi-Qing Zhu, Fu-Hao Ma, and Ning Li performed the molecular analyses. Lei Wang, Yu-Hao Zhao, Shi-Qing Zhu, and Fu-Hao Ma prepared and examined metaphase plates. Lei Wang and Xin-Xin Sun cultured and fed the worms. Lei Wang wrote the first draft of the manuscript. Guang-Wen Chen, Zi-Mei Dong, and Ronald Sluys reviewed, revised, and finalized the manuscript. All authors read and approved of the final manuscript.

Acknowledgments

This work was supported by the National Natural Science Foundation of China (grant numbers: 31570376, 32070427, 32270501, and 32200376), the Major Public Welfare Project of Henan Province (grant number: 201300311700), the Postdoctoral Research Project of Henan Province (grant number: HN2022136), and by the Puyang Field Scientific Observation and Research Station for Yellow River Wetland Ecosystem, Henan Province. We are grateful to Dr. G. A. Stocchino (University of Sassari, Italy) for sharing her knowledge and views on the karyology of the genus *Dugesia*, which greatly improved the manuscript.

Supplementary Materials

Supplementary 1. Figure S1. Phylogenetic tree obtained from ML analysis of the concatenated dataset. Numbers at nodes indicate support values (bootstrap). New species indicated in red.

Supplementary 2. Table S1. Genetic distances for COI. Highest and lowest distance values between the two new species and congeners indicated in blue and red, respectively. Green: distance value between the two new species.

Supplementary 3. Table S2. Genetic distances for ITS-1. Highest and lowest distance values between the two new species and congeners indicated in blue and red, respectively. Green: distance value between the two new species.

References

[1] E. Solà, L. Leria, G. A. Stocchino et al., "Three dispersal routes out of Africa: a puzzling biogeographical history in freshwater planarians," *Journal of Biogeography*, vol. 49, no. 7, pp. 1219–1233, 2022.

[2] Y.-H. Chen, X.-M. Chen, C.-C. Wu, and A.-T. Wang, "A new species of the genus *Dugesia* (Tricladida, Dugesiidae) from China," *Zoological Systematics*, vol. 40, no. 3, pp. 237–249, 2015.

[3] X.-Y. Song, W. X. Li, R. Sluys, S. X. Huang, S. F. Li, and A. T. Wang, "A new species of *Dugesia* (Platyhelminthes, Tricladida, Dugesiidae) from China, with an account on the histochemical structure of its major nervous system," *Zoosystematics and Evolution*, vol. 96, no. 2, pp. 431–447, 2020.

[4] L. Wang, J.-Z. Chen, Z.-M. Dong, G.-W. Chen, R. Sluys, and D.-Z. Liu, "Two new species of *Dugesia* (Platyhelminthes, Tricladida, Dugesiidae) from the tropical monsoon forest in southern China," *ZooKeys*, vol. 1059, pp. 89–116, 2021.

[5] L. Wang, Z. M. Dong, G. W. Chen, R. Sluys, and D. Z. Liu, "Integrative descriptions of two new species of *Dugesia* from Hainan Island, China (Platyhelminthes, Tricladida, Dugesiidae)," *ZooKeys*, vol. 1028, pp. 1–28, 2021.

[6] G.-W. Chen, L. Wang, F. Wu et al., "Two new species of *Dugesia* (Platyhelminthes, Tricladida, Dugesiidae) from the subtropical monsoon region in southern China, with a discussion on reproductive modalities," *BMC Zoology*, vol. 7, no. 1, p. 25, 2022.

[7] L. Wang, Y. Wang, Z. Dong, G. Chen, R. Sluys, and D. Liu, "Integrative taxonomy unveils a new species of *Dugesia* (Platyhelminthes, Tricladida, Dugesiidae) from the southern portion of the Taihang Mountains in northern China, with the description of its complete mitogenome and an exploratory analysis of mitochondrial gene order as a taxonomic character," *Integrative Zoology*, vol. 17, no. 6, pp. 1193–1214, 2022.

[8] J. Baguñà, S. Carranza, M. Pala et al., "From morphology and karyology to molecules. New methods for taxonomical identification of asexual populations of freshwater planarians. A tribute to Professor Mario Benazzi," *Italian Journal of Zoology*, vol. 66, no. 3, pp. 207–214, 1999.

[9] K. Katoh and D. M. Standley, "MAFFT multiple sequence alignment software version 7: improvements in performance and usability," *Molecular Biology and Evolution*, vol. 30, no. 4, pp. 772–780, 2013.

[10] F. Abascal, R. Zardoya, and M. J. Telford, "TranslatorX: multiple alignment of nucleotide sequences guided by amino acid translations," *Nucleic Acids Research*, vol. 38, Supplement_2, pp. W7–13, 2010.

[11] T. A. Hall, "Precision farming: technologies and information as risk-reduction tools," *Nucleic Acids Symposium Series*, vol. 734, no. 41, pp. 95–98, 1999.

[12] C. Dessimoz and M. Gil, "Phylogenetic assessment of alignments reveals neglected tree signal in gaps," *Genome Biology*, vol. 11, no. 4, p. R37, 2010.

[13] G. Tan, M. Muffato, C. Ledergerber et al., "Current methods for automated filtering of multiple sequence alignments frequently worsen single-gene phylogenetic inference," *Systematic Biology*, vol. 64, no. 5, pp. 778–791, 2015.

[14] G. Talavera and J. Castresana, "Improvement of phylogenies after removing divergent and ambiguously aligned blocks from protein sequence alignments," *Systematic Biology*, vol. 56, no. 4, pp. 564–577, 2007.

[15] R. Lanfear, B. Calcott, S. Y. W. Ho, and S. Guindon, "PartitionFinder: combined selection of partitioning schemes and substitution models for phylogenetic analyses," *Molecular Biology and Evolution*, vol. 29, no. 6, pp. 1695–1701, 2012.

[16] R. Lanfear, P. B. Frandsen, A. M. Wright, T. Senfeld, and B. Calcott, "PartitionFinder 2: new methods for selecting partitioned models of evolution for molecular and morphological phylogenetic analyses," *Molecular Biology and Evolution*, vol. 34, no. 3, pp. 772-773, 2016.

[17] F. Ronquist, M. Teslenko, P. van der Mark et al., "MrBayes 3.2: efficient Bayesian phylogenetic inference and model choice across a large model space," *Systematic Biology*, vol. 61, no. 3, pp. 539–542, 2012.

[18] A. Stamatakis, "RAxML version 8: a tool for phylogenetic analysis and post-analysis of large phylogenies," *Bioinformatics (Oxford, England)*, vol. 30, no. 9, pp. 1312-1313, 2014.

[19] K. Tamura, G. Stecher, D. Peterson, A. Filipski, and S. Kumar, "MEGA6: molecular evolutionary genetics analysis version 6.0," *Molecular Biology and Evolution*, vol. 30, no. 12, pp. 2725–2729, 2013.

[20] E. M. Lázaro, R. Sluys, M. Pala, G. A. Stocchino, J. Baguñà, and M. Riutort, "Molecular barcoding and phylogeography of sexual and asexual freshwater planarians of the genus *Dugesia* in the Western Mediterranean (Platyhelminthes, Tricladida, Dugesiidae)," *Molecular Phylogenetics and Evolution*, vol. 52, no. 3, pp. 835–845, 2009.

[21] E. Solà, R. Sluys, K. Gritzalis, and M. Riutort, "Fluvial basin history in the northeastern Mediterranean region underlies dispersal and speciation patterns in the genus *Dugesia* (Platyhelminthes, Tricladida, Dugesiidae)," *Molecular Phylogenetics and Evolution*, vol. 66, no. 3, pp. 877–888, 2013.

[22] A. Marques, I. Rossi, V. H. Valiati, and A. M. Leal-Zanchet, "Integrative approach reveals two new species of *Obama* (Platyhelminthes: Tricladida) from the south-Brazilian Atlantic Forest," *Zootaxa*, vol. 4455, no. 1, pp. 99–126, 2018.

[23] Z.-M. Dong, G.-W. Chen, H.-C. Zhang, and D.-Z. Liu, "A new species of *Polycelis* (Platyhelminthes, Tricladida, Planariidae) from China," *Acta Zoologica Academiae Scientiarum Hungaricae*, vol. 63, no. 3, pp. 263–276, 2017.

[24] L. Winsor and R. Sluys, "Basic histological techniques for planarians," in *Planarian Regeneration: Methods and Protocols*, J. C. Rink, Ed., vol. 1774 of Methods in Molecular Biology, , pp. 285–351, Humana Press, Springer Science +Business Media, 2018.

[25] G.-W. Chen, Y.-L. Wang, H.-K. Wang, R.-M. Fu, J.-F. Zhang, and D.-Z. Liu, "Chromosome and karyotype analysis of *Polycelis wutaishanica* (Turbellaria, Tricladida) from Shanxi province, China," *Acta Zootaxonomica Sinica*, vol. 33, no. 3, pp. 449–452, 2008.

[26] A. Levan, K. Fredga, and A. A. Sandberg, "Nomenclature for centromeric position on chromosomes," *Hereditas*, vol. 52, no. 2, pp. 201–220, 1964.

[27] M. Kawakatsu and J. A. Basil, "The freshwater planaria from South India," *Annotationes Zoologicae Japonensis*, vol. 48, pp. 34–42, 1975.

[28] M. Kawakatsu and G. Ôgawara, "Additional report on freshwater planarians from North Borneo, Malaya, Sri Lanka, India, and South Africa," *The Bulletin of Fuji Women's College*, no. 12, ser. II, pp. 69–86, 1974.

[29] M. Kawakatsu, I. Oki, S. Tamura, and H. Sugino, "Studies on the morphology, karyology and taxonomy of the Japanese freshwater planarian *Dugesia japonic*a Ichikawa et Kawakatsu, with a description of a new subspecies, *Dugesia japonica ryukyuensis* subspec, nov," *The Bulletin of Fuji Women's College*, no. 14, ser. II, pp. 81–126, 1976.

[30] M. Kawakatsu, I. Oki, S. Tamura, T. Yamayoshi, K. Y. Lue, and M. Hagiya, "Additional report on freshwater planarians from Taiwan," *Bulletin of Fuji Women's College*, no. 17, ser. II, pp. 59–91, 1979.

[31] M. Kawakatsu, I. Oki, S. Tamura, T. Yamayoshi, and N. Takahashi, "Morphological, karyological and taxonomic studies of *Dugesia japonica* Ichikawa et Kawakatsu from the Tsushima Islands," *Proceedings of the Japanese Society of Systematic Zoology*, vol. 19, pp. 1–10 + 2 pls, 1980.

[32] R. Sluys and I. R. Ball, "The aquatic triclads (Platyhelminthes, Tricladida) of the Bismarck Archipelago," *Steenstrupia*, vol. 16, pp. 13–20, 1990.

[33] G. A. Stocchino, R. Sluys, and R. Manconi, "A new and aberrant species of *Dugesia* (Platyhelminthes, Tricladida, Dugesiidae) from Madagascar," *ZooKeys*, vol. 425, no. 425, pp. 71–88, 2014.

[34] G. A. Stocchino, R. Sluys, M. Riutort, E. Solà, and R. Manconi, "Freshwater planarian diversity (Platyhelminthes: Tricladida: Dugesiidae) in Madagascar: new species, cryptic species, with a redefinition of character states," *Zoological Journal of the Linnean Society*, vol. 181, no. 4, pp. 727–756, 2017.

[35] G. A. Stocchino, R. Manconi, G. Corso, and M. Pala, "Karyology and karyometric analysis of an Afrotropical freshwater planarian (Platyhelminthes, Tricladida)," *Italian Journal of Zoology*, vol. 71, no. 2, pp. 89–93, 2004.

[36] I. R. Ball, "Freshwater triclads (Turbellaria, Tricladida) from the Oriental region," *Zoological Journal of the Linnean Society*, vol. 49, no. 4, pp. 271–294, 1970.

[37] T. F. Khang, S. H. Tan, S. Panha, and Z. Mohamed, "Molecular phylogenetics and sequence analysis of two cave-dwelling *Dugesia* species from Southeast Asia (Platyhelminthes: Tricladida: Dugesiidae)," *Raffles Bulletin of Zoology*, vol. 65, pp. 515–524, 2017.

[38] M. Pala, S. Casu, and R. A. Vacca, "*Dugesia hepta*, nuova specie di planaria d'acqua dolce di Sardegna appartenente alla superspecie *Dugesia gonocephala* (Dugès) (Turbellaria, Tricladida)," *Bollettino della Società Sarda di Scienze Naturali*, vol. 20, pp. 97–107, 1981.

[39] R. A. Vacca, S. Casu, and M. Pala, "Popolamento planariologico dei fiumi del Nord Sardegna. I: I cariotipi delle planarie d'acqua dolce del gruppo *Dugesia gonocephala* (Turbellaria, Tricladida) presenti nel fiume Silis (Sassari)," *Bollettino della Società Sarda di Scienze Naturali*, vol. 26, pp. 131–147, 1988.

[40] R. A. Vacca, S. Casu, and M. Pala, "Popolamento planariologico dei fiumi del Nord Sardegna. II: I cariotipi delle planarie d'acqua dolce rinvenuti nel bacino idrografico del fiume Coghinas," *Bollettino della Società Sarda di Scienze Naturali*, vol. 29, pp. 59–73, 1993.

[41] H. J. Bromley, "Morpho-karyological types of *Dugesia* (Turbellaria, Tricladida) in Israel and their distribution patterns," *Zoologica Scripta*, vol. 3, no. 5-6, pp. 239–242, 1974.

[42] M. Charni, A. H. Harrath, R. Sluys, S. Tekaya, and F. Zghal, "The freshwater planarian *Dugesia sicula* Lepori, 1948 (Platyhelminthes, Tricladida) in Tunisia: ecology, karyology, and morphology," *Hydrobiologia*, vol. 517, no. 1-3, pp. 161–170, 2004.

[43] I. Oki, S. Tamura, T. Yamayoshi, and M. Kawakatsu, "Karyological and taxonomic studies of *Dugesia japonica* Ichikawa et Kawakatsu in the Far East," *Hydrobiologia*, vol. 84, no. 1, pp. 53–68, 1981.

[44] M. Pala, R. A. Vacca, S. Casu, and G. Stocchino, "The freshwater planarian *Dugesia sicula* Lepori from Sardinia (Platyhelminthes, Tricladida)," *Hydrobiologia*, vol. 310, no. 2, pp. 151–156, 1995.

[45] G. A. Stocchino, R. Manconi, G. Corso, R. Sluys, S. Casu, and M. Pala, "African planarians: morphology and karyology of *Dugesia maghrebiana* sp. n. (Platyhelminthes, Tricladida) from Tunisia," *Italian Journal of Zoology*, vol. 76, no. 1, pp. 83–91, 2009.

[46] A. H. Harrath, R. Sluys, W. Aldahmash, A. Al-Razaki, and S. Alwasel, "Reproductive strategies, karyology, parasites, and taxonomic status of *Dugesia* populations from Yemen (Platyhelminthes: Tricladida: Dugesiidae)," *Zoological Science*, vol. 30, no. 6, pp. 502–508, 2013.

[47] P. Deri, "B-cromosomi in popolazioni polisomiche di *Dugesia benazzii* (Tricladida Paludicola) della Corsica," *Atti della Societa Toscana di Scienze Naturali, Memorie Serie B*, vol. 82, pp. 25–38, 1975.

[48] P. Deri, R. Colognato, L. Rossi, A. Salvetti, and R. Batistoni, "A karyological study on populations of *Dugesia gonocephala* s.l. (Turbellaria, Tricladida)," *Italian Journal of Zoology*, vol. 66, no. 3, pp. 245–253, 1999.

[49] E. J. de Vries, "On the karyology of *Dugesia gonocephala* s. l. (Turbellaria, Tricladida) from Montpellier, France," *Hydrobiologia*, vol. 132, no. 1, pp. 251–256, 1986.

[50] L. Leria, M. Vila-Farré, M. Álvarez-Presas et al., "Cryptic species delineation in freshwater planarians of the genus *Dugesia* (Platyhelminthes, Tricladida): extreme intraindividual genetic diversity, morphological stasis, and karyological variability," *Molecular Phylogenetics and Evolution*, vol. 143, p. 106496, 2020.

[51] L. Leria, M. Vila-Farré, E. Solà, and M. Riutort, "Outstanding intraindividual genetic diversity in fissiparous planarians (*Dugesia*, Platyhelminthes) with facultative sex," *BMC Evolutionary Biology*, vol. 19, no. 1, p. 130, 2019.

[52] S. Lorch, D. Zeuss, R. Brandl, and M. Brändle, "Chromosome numbers in three species groups of freshwater flatworms increase with increasing latitude," *Ecology and Evolution*, vol. 6, no. 5, pp. 1420–1429, 2016.

[53] M. Benazzi and G. Benazzi-Lentati, "Animal cytogenetics," in *Platyhelminthes*, vol. 1, p. 182, Gebrüder Borntraeger, Berlin, Stuttgart, 1976.

[54] A. H. Harrath, A. Semlali, L. Mansour et al., "Infertility in the hyperplasic ovary of freshwater planarians: the role of programmed cell death," *Cell and Tissue Research*, vol. 358, no. 2, pp. 607–620, 2014.